Bulletin of the Seismological Society of America, Vol. 101, No. 3, pp. 1446–1451, June 2011, doi: 10.1785/0120100143

Short Note

The Origin of Double-Frequency Microseism and Its Seasonal Variability at King Sejong Station, Antarctica

by Won Sang Lee, Dong-Hoon Sheen, Sukyoung Yun, and Ki-Weon Seo

Abstract Korea Polar Research Institute has been operating a broadband seismic station (KSJ1) at the King George Island (KGI), Antarctica, since 2001. Examining ambient seismic noise levels using power spectral analysis for the period of 2006–2008 at the KSJ1, we observed a seasonal pattern at a 4–10 s period. The amplitude of double-frequency (DF) microseism reaches a peak in May. Correlation of the DF energy and its predominant period with significant ocean-wave height and peak wave period models from the WAVEWATCH III and polarization analysis consistently indicate that ocean swell in the Drake Passage is a possible source to excite the DF microseism at the KGI. We also found that the temporal variation of DF amplitude is coincident with the seasonal change of ocean-acoustic ambient noise level around the KGI, which implies that incorporating long-term seismic and hydroacoustic noise information might give us an opportunity to figure out the characteristics of local climate variation near the Antarctic Peninsula.

Introduction

Microseisms of periods between 2 and 20 s are recorded almost anywhere in the world and vary in amplitude with the season. In general, the microseisms show two predominant peaks in the period range. A smaller amplitude, longer-period peak near 8–20 s is attributed to the direct generation of seismic waves by ocean swell at coasts. A higher-amplitude peak, double-frequency (DF) microseism near 4–10 s is generated by nonlinear ocean-wave interactions in shallow regions of the oceans that result in a frequency doubling of a standard water wave (Longuet-Higgins, 1950; Hasselmann, 1963). The DF microseism has been known to be excited by ocean waves; thus, it is likely to show seasonal variations, reflecting the vigor of ocean activities (Tanimoto, 2007), so we are able to monitor the Earth's near-surface environment using the ambient noise analysis.

Identification of the source regions of the Earth's hum, which changes seasonally, has been successfully accomplished by several studies (e.g., Rhie and Romanowicz, 2004; Bromirski and Gerstoft, 2009). In particular, Bromirski and Gerstoft (2009) showed clear correlations between ocean swell, infragravity (IG) waves and Earth's hum by comparing the hum-beam power and buoy and modeling significant wave height. This comparison enabled them to conclude that dominant source areas of the Earth's hum are near coasts. Sheen *et al.* (2009) examined seismic ambient noise recorded by broadband seismographs installed in South Korea by conducting the spectral analysis that calculates the power spectral density (PSD) of seismic noise (McNamara and Buland, 2004). They found the higher DF noise levels in winter compared with those found in summer, which is consistent with the previous results (e.g., McNamara and Buland, 2004). Recently, seasonal variations in body-wave noise have also been reported, consistent with differences in storm activity between the northern and southern hemispheres (Koper and de Foy, 2008); Gerstoft *et al.* (2008) showed that the energy of body waves (*P* waves) is also observable in the microseism spectrum from array analysis.

Although many authors have investigated seismic noise in both the northern and southern hemispheres, there are only a few studies regarding the secondary microseisms in Antarctica (e.g., Hatherton, 1960; Stutzmann *et al.*, 2009) due to a dearth of seismic stations. In this study, we analyze continuous seismic ambient noise recorded at the KSJ1 broadband seismic station, Antarctica, for the period of 2006–2008 and therefore determine the possible source region of the DF microseism, which is closely associated with the ocean swell coming from the Drake Passage (DP), using a spectral analysis method. We also show that the seasonal pattern of ambient noise might be associated with local climate variations such as a change in ice coverage in polar regions.

Data and Analysis

King Sejong station (KSS, 62.22° S/58.78° W) is located at King George Island (KGI) in the South Shetland Islands

about 100 km away from the northern Antarctic Peninsula (Fig. 1). Korea Polar Research Institute (KOPRI) has been operating a digital seismic station (KSJ1) since 2001. The KSJ1 station consists of a three-component broadband Streckeisen seismometer (STS-2).

To estimate the PSD of the seismic noise, we used a large number of 1-day-long continuous three-component seismograms during 2006–2008, with a 20 Hz sampling rate. Calculation of PSDs was conducted by following the definitive method of McNamara and Buland (2004). Then we constructed probability density functions (PDFs) from more than 40,000 of the PSDs to investigate the highest probability noise level (mode) for each channel as a function of period. In comparison with previous noise studies (e.g., Stutzman *et al.*, 2000), the method has a distinct advantage in that it does not need to screen the continuous waveforms for quiet time windows during the day. Using modes rather than higher energy levels gives us more reliable insights to determine the characteristics of ambient noise because even damaging earthquakes occurring near the station are just a small portion of the background noise in terms of occurrence.

Figure 2 exhibits a statistical view of broadband PDFs for the period of 2006–2008, and there is no significant difference between the three components except for longer periods of the east–west component. Two predominant peaks show up around 5 and 10 s in period, which correspond to secondary and primary microseisms, respectively. The standard high-noise model (HNM) and the low-noise model (LNM) (Peterson, 1993) are indicated by the gray curves in Figure 2 and are used for direct comparison with the PSD estimate in this study.

Seasonal Pattern of DF Microseism

In the PDF plot (Fig. 2) for KSJ1, we found two clear microseism peaks with a higher probability of occurrence near 5 and 10 s. Although the PDF can provide useful information on spectral signature of seismic background noise at the KGI, temporal change in the microseisms, especially the DF microseism, is barely recognized from the plot.

Because our study region is quite remote from cultural noise, we do not observe notable diurnal variation. To investigate the temporal variation of noise level, we read the statistical mode from daily PSDs so we could build a power spectrum with respect to time (Fig. 3). Interestingly, we found an annual pattern that shorter-period energy becomes weaker from July to September. This feature is prominent in 2007, whereas it seems to be rather transient in 2006 and 2008. It is coincident with the result from hydroacoustic monitoring around the KGI (Matsumoto *et al.*, 2008; Dziak *et al.*, 2010) that as the temperature drops to subfreezing and sea ice coverage reaches its maximum, the acoustic noise level declines to its seasonal minimum. This seasonal pattern observed by long-term seismic and hydroacoustic methods might be a good tool to monitor local climate change, such as ice cover variation near the Antarctic Peninsula, which is one of the fastest ice-melt regions in Antarctica. Stutzmann *et al.* (2009) also reported similar observations at the station DRV located close to Antarctica and argued that the presence

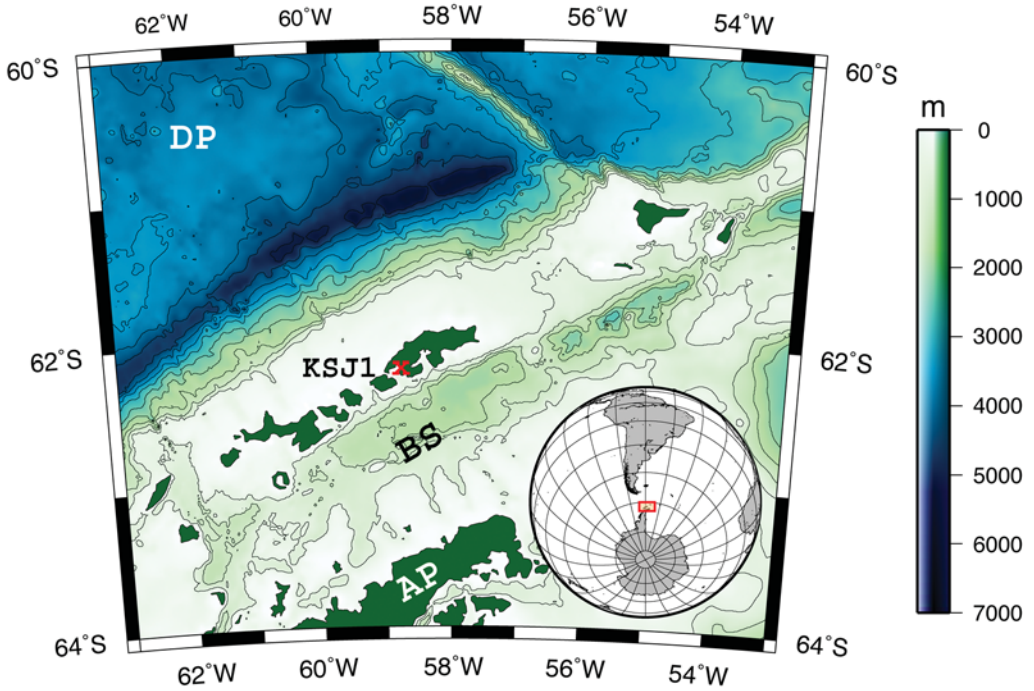

Figure 1. Location of KSJ1 installed at the King Sejong station in King George Island, Antarctica. DP, BS, and AP represent Drake Passage, Bransfield Strait, and Antarctic Peninsula, respectively.

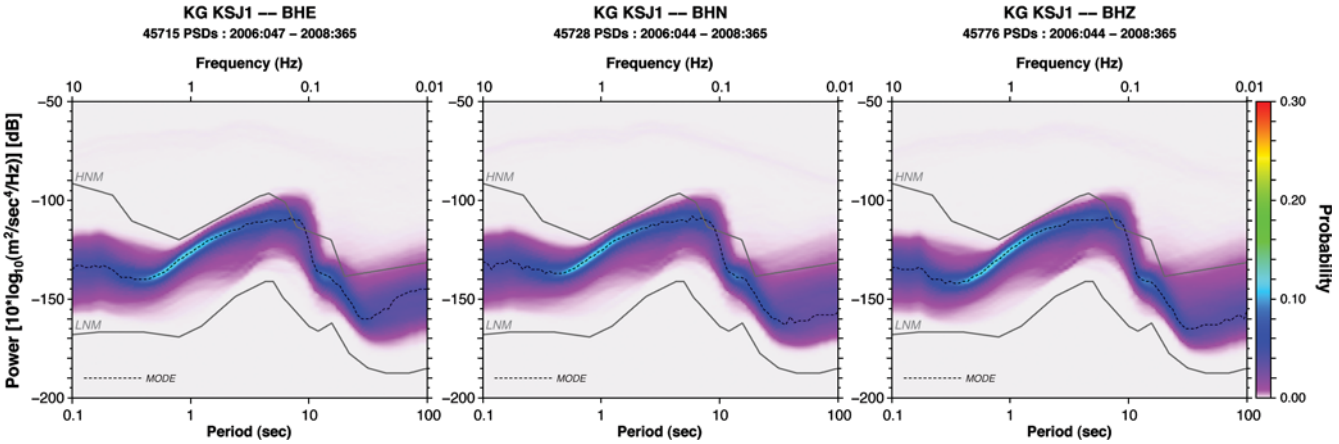

Figure 2. PDF plots of BHE, BHN, and BHZ for KSJ1 during 2006–2008. Two predominant peaks show up around 5-s and 10-s periods, corresponding to secondary and primary microseisms, respectively. HNM and LNM (gray curves) indicate the standard high-noise and low-noise models (Peterson, 1993), respectively.

of sea ice in austral winter hampers the swell reflection along the coast, causing fewer DF microseisms generated by sources.

In an attempt to carefully examine the seasonal variability of the DF microseism, we focused our interest on the period range of 4–10 s. We first calculated daily modes at each period and averaged them over the period band. There was no significant difference between east–west, north–south, and vertical components during the period of 2006–2008. Then we carried out the test of a seasonal pattern by deriving monthly averages over 3 yr, which shows an obvious seasonal variation of the DF peak (Fig. 4a, red curve). The DF energy gets to its seasonal maximum in May and tends to be weaker afterward. Ringdal and Bungum (1977) reported a pure sinusoidal pattern, which is one cycle per year, in the long-period noise level from the spectral analysis of NORSAR data for 3 yr. Rather than this, many meteorological and/or climatological factors contain a rather

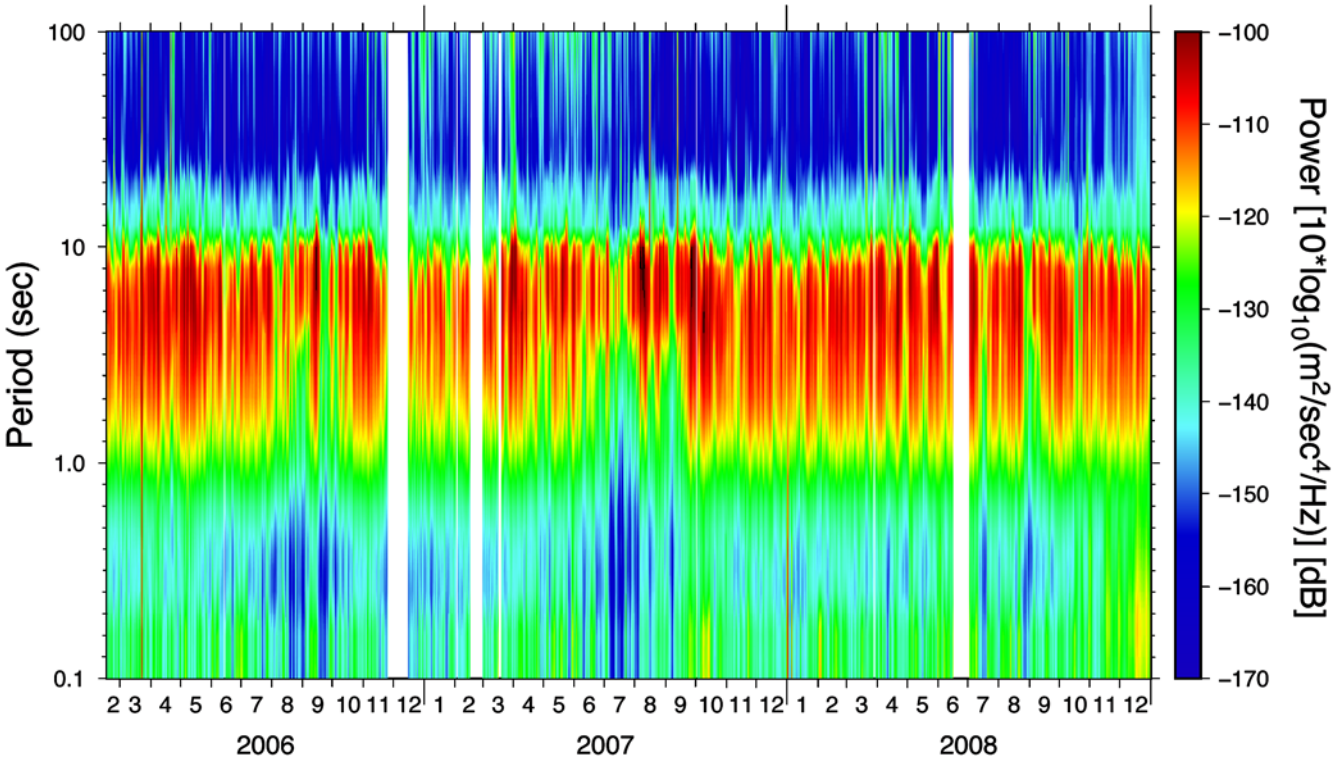

Figure 3. Seismic noise amplitude variation for the broadband vertical component (BHZ) during the period of 2006–2008. One may notice that shorter-period energy becomes weaker from July through September every year. Empty spaces in the plot indicate that data are missing.

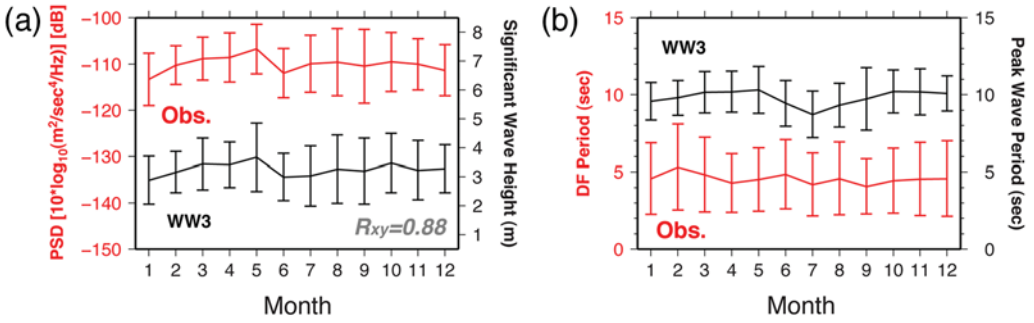

Figure 4. (a) Comparison between the amplitude (red curve with error bars) of the observed DF microseism and significant wave heights from the WW3 model in the DP (black curve). Correlation coefficient is 0.88. The curves show the seasonal maximum in May. (b) The peak wave period of the ocean swell from the WW3 in the DP (black curve) and the predominant period of DF microseisms (red curve) are about 10 s and 5 s, respectively, as predicted by our theory.

broad spectrum from one to a few cycles/year components, which show a similar seasonal pattern to that shown in Figure 4. This might be due to a regional difference between the northern and southern hemispheres. In the near future we should compile more long-period seismic noise data recorded by the other stations installed in Antarctica to find out what causes this difference.

Comparison with WW3

The seasonality of the amplitude of Earth's hum has been explained as the result of atmosphere-ocean-seafloor coupling (Rhie and Romanowicz, 2004), which shows that the northern hemisphere is strong in the winter season, whereas in the summer season, Earth's hum peaks in the southern hemisphere. Recently Bromirski and Gerstoft (2009) showed that the source of Earth's hum is coastal and revealed seasonal variation as well. As the intensity of the IG wave, in general, depends on swell amplitudes, a number of studies suggest that a distinct relation exists between wave height (Hs) and hum excitation levels, both seasonally and longer term. This is also true of the DF microseism (Sheen *et al.*, 2009). Sheen *et al.* (2009) indicated that the seasonality of the DF peak in South Korea is clear and found that several anomalous DF peaks are closely associated with the occurrence of typhoons that likely force the higher amplitude of Hs in the study region.

Ocean wave predictions are performed using the National Oceanic and Atmospheric Administration wave model WAVEWATCH III (WW3; Tolman, 2009). Significant wave height, widely used for correlation with long-period seismic noise, could be simply extracted from the WW3 (see the Data and Resources section). We collected and averaged the Hs data for a specific region, regarded as a wide enough area to effectively generate IG waves in the DP (Fig. 5). As one may notice in Figure 4a, there is apparent correlation between the DF observation and Hs with the peak cross-correlation coefficient ($R_{xy} = 0.88$) at zero lag. Both of them exhibit clear seasonal variability, having a seasonal peak in May. This tells us that the DP could be a possible contributor to the generation of the DF microseism at KGI. To validate our hypothesis, we examined peak wave period (Tp) provided by the WW3. Figure 4b represents monthly predominant periods of the DF (red curve) obtained by

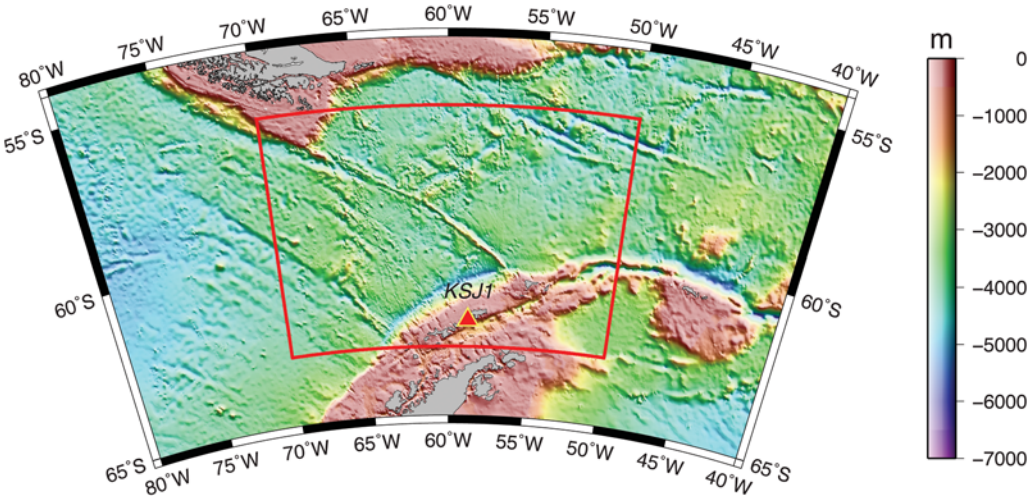

Figure 5. Sampling region (inside the red box) for collecting and averaging the Hs data in the DP, regarded as an area to effectively generate IG waves.

modes and monthly Tp (black curve). The comparison between our observation and Tp clearly explains the DF (half-period) relationship between secondary microseisms (~5 s) and peak wave periods of ocean swell (~10 s), as the theory predicted (Longuet-Higgins, 1950; Hasselmann, 1963). The results appear to confirm that ocean waves in the DP collide and generate pressure at the ocean bottom and that the pressure change generates seismic waves, which in turn, generates the DF microseism recorded at the KSJ1.

In addition to comparison with the WW3 model, we conducted polarization analysis (Jurkevics, 1988) for the three-component data to estimate source direction of the primary and secondary microseisms. We then performed a 4-hr moving average of the calculated back-azimuths with an interval of 2 hr. According to the Hs information based on the WW3 in the DP, a source region that shows the maximum amplitude of Hs varies temporally but mostly lies between the tip of South America and the Antarctic Peninsula (Stutzmann *et al.*, 2009). Figure 6 shows polarization directions of both primary (red) and secondary (blue) microseisms at KSJ1. Even though we need to use multiple seismic stations in order to better resolve the locations of microseism generation (e.g., Friedrich *et al.*, 1998; Kedar *et al.*, 2008), directional analysis using a single station may still give us an insight into figuring out the source directions of microseisms. From the results of correlation with the WW3 model and polarization analysis, we can infer that the IG wave coming from the DP would be a principal contributor to the generation of DF microseism at KGI.

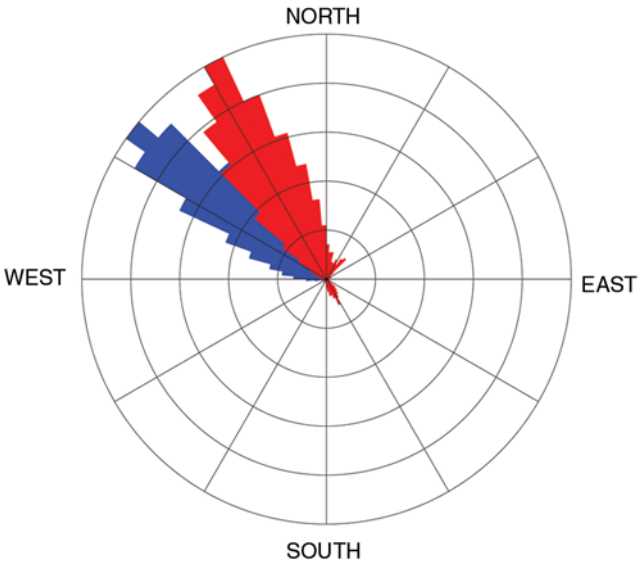

Figure 6. Direction of the microseism sources for KSJ1 during 2006–2008. Red and blue bars indicate the source directions of primary and secondary microseisms, respectively. We normalized the maximum number of occurrence for both microseisms as 1. The most abundant direction is northwest, and there is no significant seasonal variation.

Conclusions

Substantial advances in seismograph technology allow us to consistently observe the Earth's continuous oscillation everywhere in the world. The DF microseism has been known to be excited by ocean waves; thus, it is likely to show seasonal variations. Examining the ambient seismic-noise level at KSJ1, we found a seasonal pattern in the period of 4–10 s. The amplitude of the DF microseism reaches its seasonal maximum in May. Correlation of the DF peaks with significant ocean-wave height and peak wave period models indicates that the ocean swell in the DP is a possible source of excitement of the DF microseism at KGI. In addition to the spectral investigation, a polarization analysis has also shown that the source location of primary and secondary microseisms is mostly toward the DP. Comparing with the seasonal change of sea-ice coverage and the hydroacoustic ambient-noise level gives us an opportunity to link local climate change to the long-term variation of seismic ambient noise in polar regions.

Data and Resources

Seismograms used in this study were collected by KOPRI and are not yet released to public. The hindcast WW3 model can be downloaded from http://polar.ncep.noaa.gov/waves/index2.shtml (last accessed October 2009). Some plots were made using the Generic Mapping Tools version 4.3.1 (http://www.soest.hawaii.edu/gmt, last accessed October 2009; Wessel and Smith, 2008).

Acknowledgments

The authors would like to thank associate editor Charlotte A. Rowe and two anonymous reviewers for their critical comments that helped us to greatly improve the manuscript. This research was supported by KOPRI Grants PM10030, PP11010, PE10170, and PE11070.

References

Bromirski, P. D., and P. Gerstoft (2009). Dominant source regions of the Earth's "hum" are coastal, *Geophys. Res. Lett.* **36,** L13303, doi 10.1029/2009GL038903.

Dziak, R. P., M. Park, W. S. Lee, H. Matsumoto, D. R. Bohnenstiehl, and J. H. Haxel (2010). Tectonomagmatic activity and ice dynamics in the Bransfield Strait back-arc basin, Antarctica, *J. Geophys. Res.* **115,** B01102, doi 10.1029/2009JB006295.

Friedrich, A., F. Krueger, and K. Klinge (1998). Ocean-generated microseismic noise located with the Graefenberg array, *J. Seismol.* **2,** 47–64.

Gerstoft, P., P. M. Shearer, N. Harmon, and J. Zhang (2008). Global P, PP, and PKP wave microseisms observed from distant storms, *Geophys. Res. Lett.* **35,** L23306, doi 10.1029/2008GL036111.

Hasselmann, K. (1963). A statistical analysis of the generation of microseisms, *Rev. Geophys.* **1,** 177–210.

Hatherton, T. (1960). Microseisms at Scott Base, *Geophys. J. Roy. Astron. Soc.* **3,** 381–405, doi 10.1111/j.1365-246X.1960.tb01713.x.

Jurkevics, A. (1988). Polarization analysis of three-component array data, *Bull. Seismol. Soc. Am.* **78,** 1725–1743.

Kedar, S., M. Longuet-Higgins, F. Webb, N. Graham, R. Clayton, and C. Jones (2008). The origin of deep ocean microseisms in the North Atlantic Ocean, *Proc. R. Soc. A.* **464,** 777–793.

Koper, K., and B. de Foy (2008). Seasonal anisotropy in short-period seismic noise recorded in South Asia, *Bull. Seismol. Soc. Am.* **98,** 3033–3045.

Longuet-Higgins, M. S. (1950). A theory of the origin of microseisms, *Philos. Trans. R. Soc. London* Ser. A, **243,** 1–35.

Matsumoto, H., R. P. Dziak, M. Park, W. S. Lee, T. Lau, D. R. Bohnenstiehl, and J. H. Haxel (2008). Acoustic monitoring of sea ice and ice sheet off Antarctic Peninsula, *Eos Trans. AGU* **89,** no. 53, Fall Meet. Suppl., Abstract C11E-08.

McNamara, D. E., and R. P. Buland (2004). Ambient noise levels in the continental United States, *Bull. Seismol. Soc. Am.* **94,** 1517–1527.

Peterson, J. (1993). Observation and modeling of seismic background noise, *U.S. Geol. Surv. Tech. Rept. 93-322*, 1–95.

Rhie, J., and B. Romanowicz (2004). Excitation of Earth's continuous free oscillations by atmosphere-ocean-seafloor coupling, *Nature* **431,** 552–556.

Ringdal, F., and H. Bungum (1977). Noise level variation at NORSAR and its effect on detectability, *Bull. Seismol. Soc. Am.* **67,** 479–492.

Sheen, D.-H., J. S. Shin, and T.-S. Kang (2009). Seismic noise level variation in South Korea, *Geosci. J.* **13,** 183–190.

Stutzmann, E., G. Roult, and L. Astiz (2000). GEOSCOPE station noise levels, *Bull. Seismol. Soc. Am.* **90,** 690–701.

Stutzmann, E., M. Schimmel, G. Patau, and A. Maggi (2009). Global climate imprint on seismic noise, *Geochem. Geophys. Geosyst.* **10,** Q11004, doi 10.1029/2009GC002619.

Tanimoto, T. (2007). Excitation of microseisms, *Geophys. Res. Lett.* **34,** L05308, doi 10.1029/2006GL029046.

Tolman, H. L. (2009). User manual and system documentation of WAVEWATCH III version 3.14, *NOAA/NWS/NCEP/MMAB Tech. Note* **276,** 1–194.

Wessel, P., and W. H. F. Smith (2008). *The Generic Mapping Tools* version 4.3.1, released http://gmt.soest.hawaii.edu (last accessed October 2009).

Korea Polar Research Institute
504-3, Get Perl Tower, Songdo-dong, Yeonsu-gu
Incheon, 406-840, South Korea
wonsang@kopri.re.kr
(W.S.L.)

Department of Geological Environment, Faculty of Earth Systems and Environmental Sciences
Chonnam National University
Gwangju, 500-757, South Korea
(D.-H.S.)

Korea Polar Research Institute
Incheon, 406-840, South Korea
(S.Y., K.-W.S.)

Manuscript received 27 May 2010